RSC Advances

PAPER

Cite this: *RSC Adv.*, 2014, **4**, 51353

Structure and biological activity of a conformational constrained apolipoprotein A-I-derived helical peptide targeting the protein haptoglobin†

Luisa Cigliano,‡[a] Lucia De Rosa,‡[b] Donatella Diana,[b] Rossella Di Stasi,[b] Maria Stefania Spagnuolo,[c] Bernardetta Maresca,[a] Roberto Fattorusso[d] and Luca D. D'Andrea*[b]

The development of novel pharmacological treatments for atherosclerosis is an active research field in medicinal chemistry. It has been shown that the acute phase protein haptoglobin (Hpt) plays a role in modulating the reverse cholesterol transport binding to the HDL-major protein Apolipoprotein A-I, and it also plays a role in impairing the activity of the lecithin–cholesterol acyltransferase (LCAT). We reported that the peptide P2a *in vitro* and *in vivo* restores the LCAT activity in the presence of Hpt. Now, we have designed and characterized a conformational constrained P2a analogue, ApoAib, with the intention of improving Hpt binding and metabolic stability. Using non-proteogenic aminoisobutyric acid residues, we have obtained a well folded α-helical peptide with high proteolytic stability in serum. It binds to Hpt, impairs haptoglobin binding to HDL, and restores LCAT activity in the presence of haptoglobin. Furthermore, an interaction analysis using NMR revealed the peptide binding site involved in haptoglobin molecular recognition. In conclusion, ApoAib represents a promising candidate to improve reverse cholesterol transport for application in cardiovascular diseases.

Received 11th August 2014
Accepted 25th September 2014

DOI: 10.1039/c4ra08507h

www.rsc.org/advances

Introduction

Atherosclerosis is one of the human diseases with the highest mortality rate. To date, the main pharmacological treatments rely on the use of statins and the inhibition of cholesterol biosynthesis. In recent years, novel pharmacological strategies have been explored and tested in clinical trials, such as the use of niacin or the increase of high density lipoprotein (HDL) concentration.[1]

HDL is the major mediator of the reverse cholesterol transport (RCT), shuttling the cholesterol from peripheral cells to the liver for its elimination. HDL consists of phospholipids, cholesterol, triglycerides and several proteins with the prevalence of the apolipoprotein A-I (ApoA-I).[2] The clinical interest in HDL functions started when an inverse correlation was found between the HDL cholesterol levels and coronary heart diseases in the large epidemiological studies.[1a]

ApoA-I, the major protein component of HDL, is composed of 243 amino acids that fold in a prevalent all-helical structure.[3] ApoA-I stimulates the esterification of cholesterol in cholesteryl esters on the surface of circulating HDL, which is catalyzed by the enzyme lecithin–cholesterol acyltransferase (LCAT; EC 2.3.1.43). ApoA-I binds to the acute phase protein haptoglobin (Hpt).[4] In particular, Hpt recognizes the amino acid sequence 141–164 of ApoA-I.[4b] This region overlaps with the ApoA-I domain required for LCAT enzyme activation.[5] As a consequence, Hpt binding to ApoA-I impairs LCAT activity by masking the activation region of ApoA-I. The high levels of Hpt, as those circulating during the acute phase of inflammation, were suggested to be a major cause of both poor cholesterol removal from peripheral cells and reduced cholesterol uptake by hepatocytes.[4b,6]

We have investigated a novel approach that is aimed to facilitate the RCT by removing the inhibitory effect of the serum protein Hpt on the enzyme LCAT. In particular, we have explored the use of peptides interfering with Hpt–ApoA-I molecular recognition. Previously, we showed that a peptide reproducing the ApoA-I sequence 141–164, P2a, binds to Hpt and interferes with Hpt binding to ApoA-I on HDL.

[a]*Dipartimento di Biologia, Università di Napoli "Federico II", Via Mezzocannone 8, Napoli, Italy*

[b]*Istituto di Biostrutture e Bioimmagini, CNR, Via Mezzocannone 16, 80134 Napoli, Italy. E-mail: ldandrea@unina.it*

[c]*Istituto per il Sistema Produzione Animale in Ambiente Mediterraneo, CNR, via Argine 1085, Napoli, Italy*

[d]*Dipartimento di Scienze e Tecnologie Ambientali, Biologiche e Farmaceutiche, Seconda Università di Napoli, via Vivaldi 43, Caserta, Italy*

† Electronic supplementary information (ESI) available. See DOI: 10.1039/c4ra08507h

‡ These two authors contributed equally.

Furthermore, the peptide P2a restored the LCAT activity impaired by Hpt *in vitro*.[4b] Recently, we showed that P2a is also able to restore the LCAT cholesterol esterification activity *in vivo*, in an experimental mouse model of inflammation.[7] Interestingly, peptide also reduced the inflammation possibly through an HDL mediated mechanism.

P2a is a 24 mer peptide that is composed of all natural amino acids. To improve target affinity and serum stability properties of P2a peptide for *in vivo* applications, we have designed a conformational constrained P2a analogue using unnatural amino acids. In particular, we have designed a novel peptide sequence, ApoAib, using the non proteogenic and high helix inducer aminoisobutyric (Aib) amino acid.[8] The designed peptide adopts a helical conformation in water, binds to Hpt with improved affinity and preserves P2a biological activity *in vitro*. Furthermore, it shows an improved metabolic stability in serum with respect to P2a. Further, we have characterized its interaction with Hpt by NMR. This study suggests that the designed peptide is a candidate lead compound for *in vivo* experimentation in cardiovascular diseases.

Results and discussion

Peptide design

Peptide P2a reproduces the ApoA-I sequence from residue 141 to 164.[4b] The structural analysis of ApoA-I in the lipid poor or rich forms showed that the amino acid segment 141–164 is characterized by an α-helix motif,[3] suggesting that this could be the conformation recognized by Hpt. We hypothesized that P2a, which is unstructured in solution, could adopt a helical conformation when bound to Hpt by an induced fit mechanism. We reasoned that the preorganization of P2a in a helical conformation, reducing the entropic cost of the binding event, should improve the peptide binding affinity to Hpt, and therefore, its biological activity. The charged and His residues (functional residues) were preserved considering that they are highly conserved in ApoA-I sequences within homologue species,[9] and we hypothesized that they could be implicated in Hpt recognition. The design of a conformationally stable helical peptide was achieved replacing the remaining non-functional residues with the high helicogenic aminoisobutyric acid and alanine residues (Fig. S1†).[10] It was expected that the increased helical conformational stability and the use of unnatural amino acids (Aib) should also improve the peptide metabolic stability.[11] The previous studies highlighted that an excessive percentage (>50%) of Aib residues will induce a 3_{10} helix conformation.[8] We decided to introduce four Aib residues spaced by three residues (i, $i + 4$ positions) to sustain the helix formation through all the sequence. The Aib residues were inserted in position 4, 8, 12 and 16 replacing the P2a residues leucine, methionine, alanine and valine, respectively. The remaining residues (Ser2, Pro3, Gly5, Leu19 and Leu23) were replaced with alanine, the amino acid with the highest intrinsic helix propensity, whereas Leu1 was substituted with Trp to introduce a spectroscopic probe. The final sequence of the designed peptide (Fig. S1†), ApoAib, is Acetyl-Trp-Ala-Ala-Aib-Ala-Glu-Glu-Aib-Arg-Asp-Arg-Aib-Arg-Ala-His-Aib-Asp-Ala-Ala-Arg-Thr-His-Ala-Ala-NH_2.

Conformational analysis in solution

The conformational analysis of ApoAib peptide was initially performed by circular dichroism (CD) in 10 mM phosphate buffer of pH 7.3. The CD spectrum (Fig. 1) showed a double minimum at 208 and 222 nm, a crossover point at 200 nm and a well-defined maximum around 190 nm. These spectral characteristics are clearly indicative of an α-helical conformation.[12] In comparison, the CD spectrum of peptide P2a, in the same experimental conditions, showed the minimum around 200 nm, which is indicative of a almost a random coil conformation (Fig. 1).[12]

To get molecular insights on the ApoAib structure, its conformational preferences were investigated using NMR spectroscopy. Peptide aggregation state was checked acquiring mono-dimensional spectra in the concentration range 0.5–3 mM (Fig. S2†). No significant changes were observed in the distribution and in the shape of the ^{1}H resonances, indicating that no aggregation phenomena occurred in the analyzed concentration range. The sequential assignment approach, based on homonuclear 2D 1H NMR,[13] was used to obtain complete sequence specific ^{1}H NMR assignment (Table S1†). The identification of spin systems and resonance assignment were established by a combination of two-dimensional DQF-COSY and TOCSY spectra, while sequence-specific assignment was obtained by a NOESY experiment. The Hα chemical shifts analysis performed using chemical shift index[14] (Fig. 2) suggested a high helical propensity of the central region of the peptide. Two-dimensional NMR NOESY spectrum showed a high number of cross peaks. All short- and medium-range NOE effects involving the backbone protons of ApoAib are summarized in Fig. S3a.† The whole sequence is characterized by sequential NH_i–NH_{i+1} NOEs, which are typical of a helical structure. In particular, (i, $i + 2$) and (i, $i + 3$) NOE effects were observed for the entire stretch of residues 6–18. The N- and C-terminal regions lack a regular NOE pattern, thus suggesting a prevalence of disordered structures.

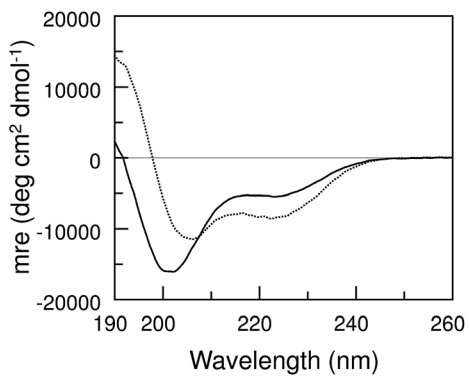

Fig. 1 Circular dichroism spectra of peptide ApoAib (dotted line) and P2a (solid line) in 10 mM phosphate buffer pH 7.3. (mre = mean residue ellipticity).

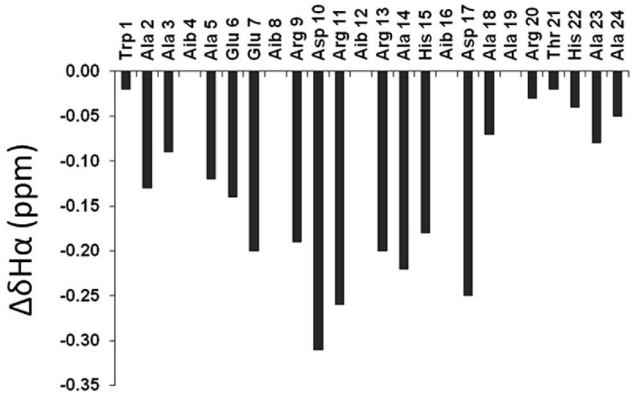

Fig. 2 Hα chemical shift differences plotted for the 24 residues of ApoAib. Negative Hα chemical shifts are indicative of a helical conformation.

Three-dimensional structures were calculated by simulated annealing in torsion angle space and restrained molecular dynamics methods based on NOE-derived restraints using the CYANA software package.[15] The final data set (Table 1) for the calculation of the ApoAib structure consisted of a total of 260 NOE constraints (123 intra-residue, 91 short-range, 44 medium-range and 2 long-range) and 81 torsional angle restraints. The backbone overlay of the best 20 CYANA conformers displays a good convergence confirmed by a backbone and all heavy atoms root-mean-square difference (rmsd) values of 0.27 ± 0.10 Å and 1.18 ± 0.15 Å, respectively (Fig. S4a†). Consistent with the chemical shift index data and with the NOE patterns, the NMR calculated models showed the presence of significantly regular structures in the central region with frayed N- and C-termini (residues 1–5 and 19–24). The analysis of φ and ψ dihedral angles (Fig. S5a†), associated with the (i, i + 4) pattern of hydrogen bonds (Table S2†), confirms that the peptide sequence 6–18 adopts a regular α-helix conformation.

The spectroscopic characterization of ApoAib peptide in solution showed that the introduced amino acid substitutions stabilize the α-helix conformation without distortion towards a 3_{10} helix. This structural motif should constrain the interacting residues in the favorable three dimensional arrangements to interact with Hpt. Further, the peptide conformational pre-organization should increase the affinity to the target, reducing the binding entropic cost.

Table 1 Structural statistics of the final 20 NMR structures of the ApoAib free and bound to Hpt protein

	ApoAib free	ApoAib bound
No. of the distance restraints		
Unambiguous NOE	260	286
Ambiguous NOE	95	101
Total NOE	355	387
Divided into		
Intra-residue NOE	123	131
Sequential NOE	90	98
Medium range NOE	44	52
Long range NOE	2	5
Residual NOE violations		
Number > 0.1°	±1	±1
Maximum, Å	0.18 ± 0.02	0.12 ± 0.03
Residual angle violations		
Number > 2.0°	0 ± 0	0 ± 0
Maximum, Å	0	0
Amber energies, kJ mol^{-1}		
Total	−288 ± 15	−300 ± 19
Van der Waals	−105 ± 12	−120 ± 10
Electrostatic	−212 ± 18	−258 ± 22
R.m.s.d[a] (Å) to a mean structure		
Backbone residues (4–20)	0.27	0.15
Heavy atoms residues (4–20)	1.18	0.99
Ramachandran plot residues[b] (%)		
In most favored regions	44.5	75.0
In additional allowed regions	40.0	24.0
In generously allowed regions	14.5	0.5
In disallowed regions	1.0	0.5

[a] Calculated by MOLMOL. [b] Calculated by CYANA 2.1.

NMR analysis of ApoAib–Hpt interaction

The interaction between the ApoAib peptide and Hpt protein was investigated combining saturation transfer difference (STD)[16] and trNOESY experiments.[17] First, the one-dimensional STD NMR experiments of ApoAib peptide in the presence or absence of Hpt were carried out to identify the peptide residues involved in Hpt binding. The ApoAib signals were present in the STD NMR spectrum in the presence of Hpt (Fig. 3a and b), but they were absent in the control experiment (data not shown); this suggests the formation of the complex ApoAib–Hpt. The STD NMR spectral region, corresponding to the amide protons, is well resolved, and it can be used to classify the residues that are relevant for the interaction with the Hpt protein. The relative degree of saturation for individual protons, normalized to the amide proton of Arg13, was used to compare STD effects and identify peptide binding residues (Fig. 3c).[16a] The analysis of the STD spectrum showed that H_N resonances of the E6, R9, R13 and R20, along with the H_ε side chains resonances of residues R9, R13 and R20, have STD intensities between 60% and 100%, suggesting that these residues have tighter contacts with the protein surface. In addition, the H_N protons of the residues D10 and D17 showed evident enhancements (>50%), indicating a probable involvement of these residues in protein recognition.

The Hpt-bound conformation of ApoAib was investigated by trNOESY experiments at a peptide–protein molar ratio of 100 : 1.[18] Because of the low peptide–protein molar ratio, free and bound peptide molecules were involved in a fast chemical exchange, and only a single set of resonances were observed. In particular, a large number of additional trNOE cross peaks were observed in the presence of the protein target. These include trNOESY connectivities involving the side chain protons of E6, R9, D10, R13, D17 and R20, as well as the side chain protons of the above residues with the main backbone protons, suggesting

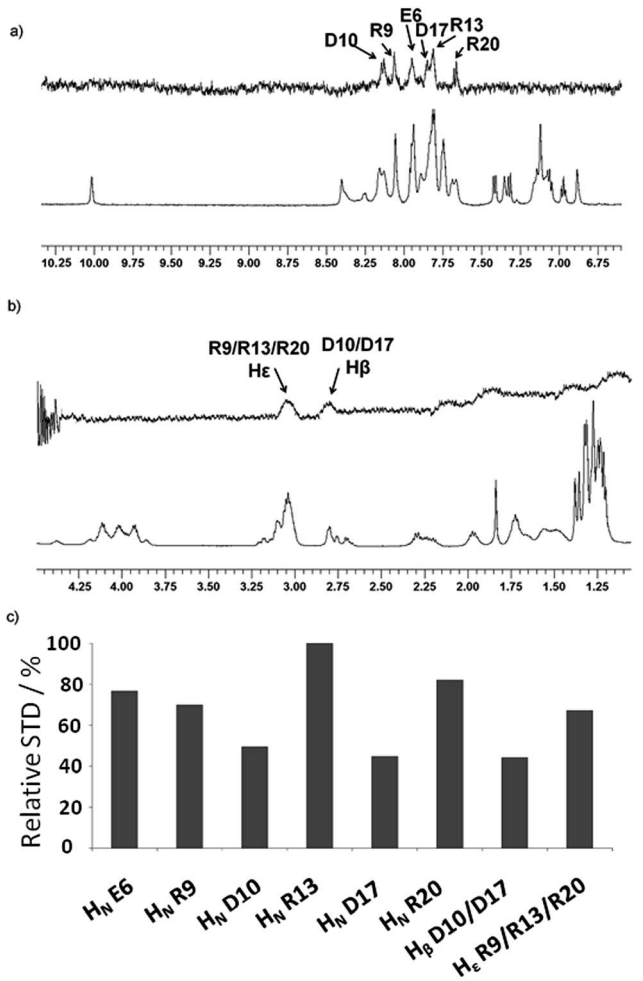

Fig. 3 (a) Low field region of the reference 1D ^{1}H spectrum (bottom) and 1D ^{1}H STD NMR spectrum (top) of 1 mM ApoAib in the presence of 10 μM Hpt. (b) Aliphatic region of the reference 1D ^{1}H spectrum (bottom) and 1D ^{1}H STD NMR spectrum (top) of 1 mM ApoAib in the presence of 10 μM Hpt. Residues showing the strongest STD effects are highlighted. (c) Relative STD intensities (in percent) of the protons of the residues showing more enhancements of the resonances in the ^{1}H STD spectra.

that these side chains are more constrained in the bound state. Indeed, the addition of Hpt caused a soft line broadening, especially observable on the amide and side chain protons of residues R9, R13, and R20. Moreover, a very slight chemical shift difference relative to the free peptide was also detected for the amide protons of R9, R13, and R20. These two effects, line broadening and chemical shift perturbations, which occurred on the proton of the same residues, confirmed the existence of the binding. This evidence is also confirmed by a pattern of additional intense and medium NOE connectivity in C- and N-termini (Fig. S3b†). To determine the conformation of the bound state of ApoAib, a total of 286 trNOE experimental distance constraints (131 intra-residue, 98 short-range, 52 medium-range and 5 long-range) were incorporated into a simulating annealing protocol (Table 1). A set of 20 lowest energy structures generated by CYANA software in the final iteration was subjected to energy minimization, followed by checks for the correct geometry and agreement with distance restraints. The average rmsd for the superimposition of the 20 bound structures with lowest-energy (Fig. S4b†) from residue 4 to 20 was 0.15 ± 0.09 Å for the backbone atoms, and 0.99 ± 0.11 Å for the all heavy atoms. The calculated structures comprise a regular α-helix encompassing the entire peptide sequence, in agreement with NOE data, H-bonding (Table S3†) and pattern of φ/ψ angles (Fig. S5b†). This structure presents the interacting residues, as determined by STD-NMR, on the same face of the helix (Fig. 4). The combination of ApoAib epitope characterization, as derived by the STD experiments, with the determination of ApoAib free and bound conformation obtained by trNOESY experiments allowed us to get relevant molecular details of the interaction between ApoAib and Hpt. This structural analysis clearly shows that the binding to Hpt requires ApoAib to adopt a helical conformation encompassing virtually the entire peptide sequence; in particular, the protein binding triggers a significant helix elongation, supporting the hypothesis that P2a binding could be improved by inducing suitable conformational pre-organization. Interestingly, the ApoAib residues involved in Hpt binding (E6, R9, D10, R13, D17 and R20) correspond to a highly conserved ApoA-I charged residues.

Analysis of ApoAib binding to haptoglobin

To evaluate the binding efficiency of ApoAib to Hpt, in comparison with P2a, different amounts (1, 3, 10 or 30 μM) of biotinylated peptides were loaded into Hpt-coated wells

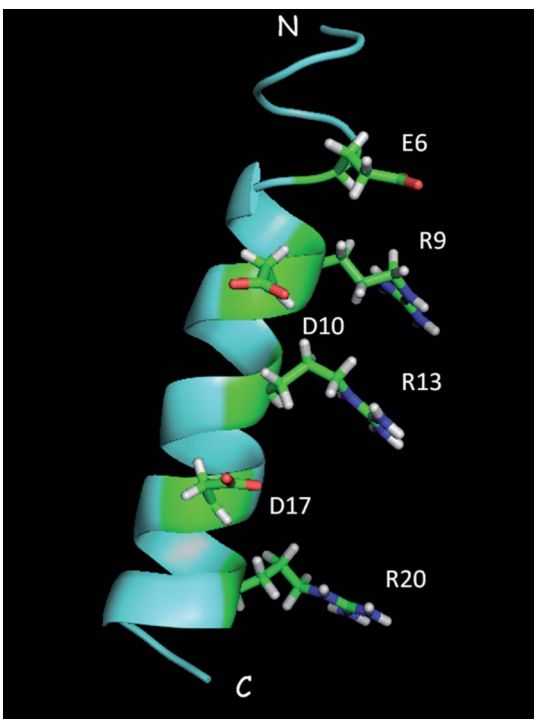

Fig. 4 View of the lowest energy structure of the bound ApoAib. The side chains of the residues with the strongest STD amplification factor are displayed as neon.

(Fig. 5). ApoAib peptide was able to bind to Hpt in a dose-dependent manner, and it showed a higher binding efficiency than P2a at any assayed concentration ($p < 0.01$). Because Hpt has been reported to capture free haemoglobin (Hb) for its elimination by liver,[19] we investigated whether ApoAib binding to Hpt interferes with the Hb-capturing function of Hpt. ApoAib does not compete with Hb for binding with Hpt at any assayed concentration; thus, demonstrating that the ability of Hpt to interact with Hb is retained in the presence of ApoAib (Fig. S6†).

These data suggest that the helical preorganization induced by the Aib residues improves the peptide binding to Hpt without impairing Hb-binding, and therefore, Hpt physiological activity is also retained.

Competition of ApoAib peptide with HDL for binding Hpt

Hpt binds to ApoA-I, which is displayed on the surface of HDL. To investigate the biological properties of ApoAib, its ability to influence the Hpt binding to HDL was *in vitro* evaluated and compared to P2a. HDL-coated wells were incubated with 1 μM Hpt in the absence or presence of different amounts (0.3 to 10 μM) of P2a or ApoAib, and the amount of HDL-bound Hpt was measured. As shown in Fig. 6, the inhibition of Hpt binding to HDL by ApoAib was higher than those of P2a when the two peptides were used at concentration of 0.3–3 μM ($p < 0.01$), and they did not differ when used at 10 μM concentration. In particular, P2a significantly impaired Hpt interaction with HDL ($p < 0.01$) only at a concentration higher than 1 μM, while ApoAib was able to displace Hpt from HDL binding ($p < 0.01$) at any assayed concentration. These results confirm that ApoAib has an enhanced ability with respect to P2a to bind to Hpt, and an improved capacity to interfere with the binding between Hpt and HDL.

Effect of ApoAib on LCAT inhibition by Hpt

The ability of the peptides to compete with ApoA-I for binding Hpt was also evaluated in an LCAT activity assay. Dextran sulfate-treated plasma and labeled proteoliposomes (LCAT and ApoA-I-containing cholesterol sources, respectively) were incubated with 1 μM Hpt in the absence or presence of different amounts (1 to 4 μM) of each peptide. The LCAT activity was significantly reduced (about 50%) by Hpt (6.6 ± 0.2 units *vs.* 3.3 ± 0.2 units; $p < 0.0001$), but restored when peptides were present during incubation (Fig. 7), with ApoAib being effective as P2a ($p < 0.0001$) in rescuing the enzyme activity. In particular, the use of 4 μM ApoAib in the assay completely restored the enzyme activity. Indeed, the two peptides completely saved the

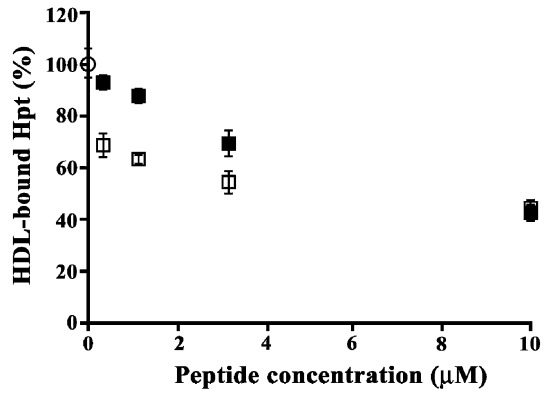

Fig. 6 Peptide competition with HDL for binding with Hpt. Hpt (1 μM) was incubated for 2 h at 37 °C with acetylated P2a (full squares), or ApoAib (open squares) (0 to 10 μM). Aliquots were then incubated in HDL-coated wells (2 h, 37 °C). Hpt binding to HDL was detected by rabbit anti-Hpt IgG and GAR-HRP IgG. The amount of immunocomplexes was determined by measuring the absorbance at 492 nm. Data are reported as the percent of the value obtained by the incubation of Hpt alone (open circle), and expressed as mean ± SEM.

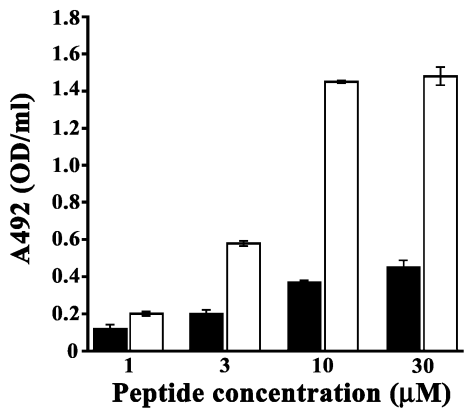

Fig. 5 Binding of ApoAib or P2a to Hpt. Different concentrations (1, 3, 10, or 30 μM) of biotinylated P2a (full bar) or ApoAib (open bar) were incubated in Hpt-coated wells. Avidin-HRP was used to detect bound peptides. The samples were analyzed in triplicate and the data are expressed as mean ± SEM.

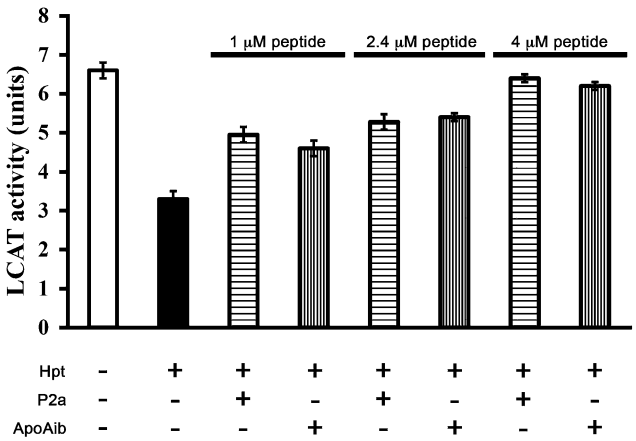

Fig. 7 Effect of ApoAib on the inhibition of LCAT activity by Hpt. The LCAT activity was assayed in the absence or presence of 1 μM Hpt and different amounts (1, 2.4 or 4 μM) of P2a or ApoAib. A pool of plasma samples (treated with 0.65% dextran sulphate, MW = 50 kDa, in 0.2 M $CaCl_2$ to remove lipoproteins) was used as the source of LCAT, while a proteoliposome (ApoA-I–lecithin–^{3}H-cholesterol, 1.5 : 200 : 18 molar ratio) was used as the substrate. The LCAT activity is expressed in units corresponding to nmol of cholesterol incorporated per hour per mL of plasma. Samples were analyzed in triplicate, and data are expressed as means ± SEM.

enzyme stimulation by ApoA-I, when used at 4 μM concentration in the assay (peptide–Hpt molar ratio 3 : 1.). The peptides, when incubated without Hpt, did not significantly affect the cholesterol esterification (Fig. S7†).

Serum stability analysis

Finally, the proteases stability of ApoAib peptide in human serum was evaluated. The amount of peptide was determined by HPLC by evaluating the area of the ApoAib peak, which was revealed at 210 nm after 4 hours of incubation time in 100% serum (Fig. S8a†). The peptide ApoAib retained the 88 ± 6% of its initial amount suggesting good overall proteolytic stability. In comparison, the P2a peptide, in the same experimental conditions, was almost completely degraded, retaining only 41 ± 8% of the initial amount (Fig. S8b†). The identity of the remaining ApoAib peptide was verified by LC-MS after 6 hours of incubation (Fig. S8c†). This result suggests that ApoAib shows a good overall metabolic stability, and the substantial proteases stability increase with respect to P2a.

Conclusions

ApoAib is a helical constrained peptide with high serum proteases resistance and improved Hpt-binding efficiency. ApoAib binds to Hpt in a helical conformation, mainly using a stretches of charged residues located on the side of the helix as highlighted by NMR spectroscopy. ApoAib binds to Hpt and efficiently restores the LCAT activity in the presence of Hpt. In conclusion, we characterized the biological activity and the molecular recognition properties at atomic level of the peptide ApoAib, which is a novel candidate to improve reverse cholesterol transport with application in cardiovascular diseases.

Experimental section

Chemicals

Fmoc protected amino acids and coupling reagents were purchased from Iris-Biotech (Marktredwitz, Germany). PAL-PEG PS resin was obtained from Applied Biosystems (Life Technologies Italia, Monza. Italy). Peptide synthesis solvents (DMF, NMP and DCM) and acetonitrile were supplied by Romil (Cambridge, UK) and used without further purification; DIPEA, acetic anhydride, piperidine, TIS and diethyl ether were obtained from Sigma-Aldrich (Milan, Italy).

Biochemicals

Chemicals of the highest purity, bovine serum albumin fraction V (BSA), human serum albumin (HSA), cholesterol, rabbit anti-human Hpt IgG, goat anti-rabbit horseradish peroxidase-conjugated (GAR-HRP), *o*-phenylenediamine (OPD), Avidin-HRP, and molecular weight markers were purchased from Sigma-Aldrich (St. Louis, MO, USA). Human HDL was obtained from Merck Millipore (Darmstadt, Germany). [1α, 2α-3H] Cholesterol (45 Ci mmol^{-1}) was obtained from Perkin Elmer (Boston, USA). Polystyrene 96-wells ELISA MaxiSorp plates from Nunc (Roskilde, Denmark), and Sil-G plates for thin-layer chromatography (0.25 mm thickness) of Macherey-Nagel (Düren, Germany) were used. Sephacryl S-200, CNBr-activated Sepharose 4 Fast Flow and Blue Sepharose 6 Fast Flow resins were obtained from GE-Healthcare Life Sciences (Milano, Italy).

Peptide synthesis

All the peptides were synthesized on a solid phase using an Fmoc-Pal-PEG-PS resin (0.42 mmol g^{-1}) and standard Fmoc chemistry. Each coupling reaction was performed for 1 h using 10 equivalents of the Fmoc-protected amino acid, 9.9 equivalents of hydroxybenzotriazole (HOBt)/*O*-benzotriazole-*N*,*N*,*N*′,*N*′-tetramethyl-uronium-hexafluoro-phosphate (HBTU) and 20 equivalents of the base DIPEA. The removal of Fmoc was carried out by incubating the resin with a solution of 30% v/v piperidine in DMF twice for 5 minutes. After each coupling, unreacted N-terminal amino groups were capped with a solution of 2 M acetic anhydride, 0.06 M HOBt, 0.55 M DIPEA in DMF (5 min). Each step was followed by five washing with DMF for 1 min. Peptides were labeled with biotin on a solid phase on the N-terminal amino group. The biotinylation reaction was performed with 3 eq. of biotin–carboxamido–hexanoic acid (Sigma-Aldrich, Milan, Italy) in the presence of 3 eq. of *N*,*N*,*N*′,*N*′-tetramethyl-*O*-(7-azabenzotriazol-1-yl)uronium hexafluorophosphate (GL Biochem, Shanghai, China) and 6 eq. of DIPEA. Peptide cleavage from the resin and amino acids side-chain deprotection were achieved by treatment with TFA, triisopropyl silane and water (95 : 2.5 : 2.5) at room temperature for 3 h. Cold diethyl ether was used to precipitate the peptide. Crude products were collected by centrifugation, resuspended in a water–acetonitrile mixture and lyophilized. The peptide were purified by reverse-phase HPLC on a Shimadzu LC-8A instrument equipped with an SPD-M10 AV detector using a C18 column Jupiter (250 × 10 mm, 300 Å, 10 μm; Phenomenex, Torrance, USA) and a gradient of CH_3CN (0.1% TFA) in H_2O (0.1% TFA) from 5% to 70% in 20 min. Peptide purity (>95%) and identity were verified by RP-HPLC and-MS analysis on an Agilent 1200 Infinity Series (Agilent Technologies, Santa Clara, USA) equipped with a diode array and an ESI-ToF detector using a C18 column (Jupiter 150 × 2.0 mm, 300 Å, 3 μ; Phenomenex, Torrance, USA) and a gradient of CH_3CN (0.1% TFA) in H_2O (0.1% TFA) from 5% to 70% in 20 min. The peptide final yield was 17%.

ApoAib: MW_{calc} 2641.3334 Da; MW_{exp}: 2641.3584 Da. t_R = 14.3 min.

P2a: MW_{calc}: 2754.4460 Da; MW_{exp}: 2754.4773 Da. t_R = 14.9 min.

Serum stability assay

A 500 μL total human serum (Sigma-Aldrich, Milan, Italy) aliquot was thawed at 4 °C and centrifuged at 13 200 rpm at 4 °C for 10 min. Supernatant was recovered and incubated at 37 °C for 10 min in a water bath. Lyophilized ApoAib or P2a peptides were dissolved in sterile water at a concentration of 6.8 mg mL^{-1} and centrifuged at 13 200 rpm for 5 min at 4 °C. Supernatants were recovered and peptides were diluted to 0.5 mg mL^{-1} with activated human serum in a total volume of

100 μL. After zero and 4 h of incubation at 37 °C, 10 μL of reaction mixture were diluted with 90 μL of water (TFA 0.1%) and centrifuged at 4 °C for 5 min. The supernatant (50 μL) was analyzed by RP-HPLC (Waters Alliance HT) on a Jupiter 4u Proteo (150 × 4.6 mm, Phenomenex), using a linear gradient of CH_3CN (0.1% TFA) in water (0.1% TFA) from 5% to 70% in 20 min. The amount of remaining peptide was determined evaluating the area of the HPLC peak revealed at 210 nm. The percentage of remaining peptide was estimated by comparing the peak area at 0 and 4 hours. Experiments were carried out in triplicate.

Circular dichroism spectroscopy

CD spectra were collected at 20 °C in the wavelength range of 260–190 nm using 0.1 mm path-length quartz cuvette (Hellma, Milan, Italy) on a Jasco 720 instrument (Easton, MD, U.S.) using the following parameters: scanning speed 10 nm min^{-1}, bandwidth 1.0 nm, data pitch 0.1 nm, response 4 s, and five spectra accumulations. All the experiments were performed in 10 mM phosphate buffer, pH 7.3, at a peptide concentration of 50 μM for ApoAib and 74 μM for P2a. Peptides were dissolved in filtered and degassed water and then diluted to the final concentration using buffer solution. ApoAib concentration was determined by absorbance at 280 nm using a molar extinction coefficient of 5500 M^{-1} cm^{-1}, whereas P2a peptide was quantified according to Anthis and Clore.[20] CD spectra are displayed in mean residue ellipticity.

NMR measurements

The ^1H NMR spectra of the free peptide were recorded at 1 mM sample concentration in 50 mM sodium phosphate buffer at pH 7.0 in 90% H_2O and 10% ^2H_2O. The ^1H NMR spectra were run at 298 K on a Varian INOVA 600 MHz spectrometer equipped with a cold probe. All the experiments were carried out using the double pulsed gradient spin-echo (DPSGE) to eliminate the solvent signal in $H_2O/^2H_2O$ solution. The conventional two dimensional experiments TOCSY, NOESY and DQF-COSY spectra were recorded at 298 K. TOCSY spectra were recorded with a mixing time of 70 ms, while for NOESY experiments an optimal mixing time of 250 ms was observed in the 50–500 ms range. Spectra were acquired at 8 scans/t1 increment for TOCSY and with 32 scans/t1 increment for NOESY. DQF-COSY was acquired with 4096 data points in F2 dimension and 500 increments with 64 scans to obtain a suitable resolution to measure $^3J_{HNH\alpha}$ coupling constants. The one-dimensional STD-NMR[16a] spectrum of the Hpt–peptide was performed at 600 MHz and 298 K with 1024 scans and a relaxation delay of 2.0 s. The NMR sample of peptide in the presence of the Hpt contained 0.01 mM protein and 1.0 mM peptide for a protein–peptide ratio of 1 : 100. STD spectra were recorded with a selective saturation of protein resonances with *on-resonance* at 12 ppm or −1 ppm and *off-resonance* irradiation at 30 ppm for reference spectra. A series of 40 Gaussian shaped pulses were used for a total saturation time of 2.0 s. The 1D STD spectra were obtained by the internal subtraction of saturated spectra from reference spectra by phase cycling. Relative STD values were calculated by dividing STD signal intensities by the intensities of the corresponding signals in a one-dimensional ^1H NMR reference spectrum of the same sample, and it was similarly processed. Transferred nuclear Overhauser effect (trNOESY)[17] spectra of the Hpt–peptide complex were recorded with 4k points and 512/t1 increments, and a relaxation delay of 1.5 s. The optimal conditions for the trNOESY measurements were determined by considering a peptide–Hpt molar ratio ranging from 10 to 100 with mixing times of 50, 100, 200, 300 and 500 ms. After the optimization of the peptide–Hpt ratio, the final NMR sample was prepared with 1.0 mM of peptide and 0.01 mM of protein, which corresponds to a protein–peptide ratio of 1 : 100 in 500 μL of buffer solution at pH 7.0. Structure calculations were based on a spectrum recorded with a mixing time of 200 ms. All the spectra were processed with software Sparky[21] and analyzed with Neasy,[22] a tool of computer aided resonance assignment (CARA) software. Structure calculations were performed with the program CYANA version 2.1.[15] The NOE cross peak intensities were used to obtain distance constraints. The ϕ angle restraints were derived from $^3J_{HNH\alpha}$ coupling constants. Structure calculations were initiated from 100 random conformers; the 20 structures with the lowest CYANA target functions were analyzed with the programs MOLMOL[23] and Pymol (http://www.pymol.org/), and they were further refined using the program SPDB VIEW.[24] A total of 600 steps of steepest descent minimization, using the Gromos 96 force field,[25] were applied to each of the 20 structures over three steps.

Purification of Hpt

Hpt was isolated from the plasma of healthy subjects (phenotype 2-1, 2-2, or 1-1) by a multi-step purification procedure based on a gel filtration with a column of Sephacryl S-200, followed by affinity chromatography with a column of Blue Sepharose 6 Fast Flow, and finally by further purification by affinity chromatography using a Sepharose resin coupled to anti-Hpt IgG.[6] Hpt was over 98% pure, as assessed by the SDS-PAGE and densitometric analysis of Coomassie-stained bands. The molarity of each Hpt phenotype was determined by measuring the protein concentration[26] and calculating the molecular weight of the monomer αβ, as previously described.[27]

ELISA experiments

ELISA was essentially performed as previously reported.[4b,28] In particular, experiments of peptides binding to Hpt were performed by incubating the wells with of 0.5 μg of Hpt in 50 μL of coating buffer (7 mM Na_2CO_3, 17 mM $NaHCO_3$, 1.5 mM NaN_3, pH 9.6). After four washes by TBS (130 mM NaCl, 20 mM Tris–HCl, pH 7.4) containing 0.05% (v/v) Tween 20 (T-TBS) and four washes by high salt TBS (500 mM NaCl in 20 mM Tris–HCl at pH 7.4), the wells were blocked with TBS containing 0.5% BSA (1 h, 37 °C). The wells were then incubated (1 h, 37 °C) with 55 μL of biotinylated peptide (1, 3, 10, or 30 μM). Bound peptides were then incubated (1 h at 37 °C) with 60 μL of Avidin-HRP diluted to 1 : 10 000. Peroxidase-catalysed colour development from *o*-phenylenediamine was measured at 492 nm.[29] Competition experiments were performed by coating the wells with 0.5 μg of

HDL diluted as described above. A mixture of Hpt (1 μM) with acetylated peptides embedded into proteoliposomes (0.3, 1, 3, or 10 μM peptide concentration) in CB-TBS buffer (5 mM $CaCl_2$, 0.2% BSA, 130 mM NaCl, 20 mM Tris–HCl, pH 7.3) was kept for 2 h at 37 °C, and then, incubated in the wells (2 h, 37 °C). Hpt binding was detected by treatment with 60 μL of rabbit anti-Hpt IgG (1 : 1500 dilution T-TBS containing 0.25% BSA; 1 h, 37 °C) followed by GAR-HRP-linked IgG (1 : 4500 dilution, 1 h, 37 °C). Color development was monitored at 492 nm. Absorbance values were converted to the percentage of Hpt binding in the absence of acetylated peptide.

The acetylated P2a and ApoAib peptides were embedded into proteoliposomes (peptide : lecithin : cholesterol, 1.5 : 200 : 18 molar ratio) prepared by the cholate dialysis technique.[28] In detail, egg lecithin in ethanol was mixed with cholesterol in ethanol into a glass vial. The solvent was evaporated under a nitrogen stream, and dried lipids Tris-saline (85 mM sodium cholate, 150 mM NaCl, 10 mM Tris–HCl, pH 8) was added. After vigorous whirling, the micelle suspension was incubated (90 min, 37 °C) and repeatedly shaken until clear. Then, peptide was added to the lipid suspension, which was further incubated for 1 h at 37 °C. The resulting proteoliposome suspension was extensively dialyzed against TBE (140 mM NaCl, 1 mM EDTA, 10 mM Tris–HCl, pH 7.3) at 4 °C to remove cholate.

In competition experiments of ApoAib with Hb for Hpt binding, the wells were coated with 1 μg of Hb in 50 μL of coating buffer (overnight, 4 °C). After four washes by T-TBS and four washes by high salt TBS, the wells were blocked with TBS containing 0.5% BSA (1 h, 37 °C). Mixtures of Hpt (1 μM) with different amounts (0, 3, 10, or 30 μM) of acetylated peptide, in CB-TBS buffer, were kept for 2 h at 37 °C, and then, incubated in Hb-coated wells (2 h, 37 °C). The binding of Hpt to Hb was detected by anti-Hpt IgG, GAR-HRP-linked IgG, and color development at 492 nm, as described above.

LCAT assay

LCAT activity was assayed in the absence or presence of 1 μM Hpt and 1, 2.4, or 4 μM P2a or ApoAib.[28] A pool of plasma samples, treated with 0.65% DS (MW = 50 kDa) in 0.2 M $CaCl_2$ to remove lipoproteins, was used as the source of LCAT (DS-treated plasma). The enzyme activity was essentially measured using a proteoliposome (ApoA-I–lecithin–cholesterol = 1.5 : 200 : 8 molar contribution) as the substrate according to the published procedures.[4b,30] Control assays were performed without Hpt and peptides, or in the presence of Hpt. The enzyme activity was expressed in units (nmol of cholesterol esterified per hour per mL of plasma).

Statistical analysis

ELISA was carried out with three replicates. Samples in the LCAT assay were analyzed in triplicate. The data were expressed as mean value ± SEM. The program GraphPad Prism 5.01 (GraphPad Software, San Diego, CA) was used to evaluate the significance of statistical differences by one-way ANOVA, followed by Tukey's test for multiple comparisons.

Acknowledgements

We would like to thank Mr L. Zona, M. Amendola and G. Sorrentino for technical assistance. This work was supported by the grant FIRB RBAP114AMK by MIUR to L.D.D. D.D. thanks the grant FIRB RBFR12WB3W_002 by MIUR for support.

References

1 (*a*) T. Joy and R. A. Hegele, Is raising HDL a futile strategy for atheroprotection?, *Nat. Rev. Drug Discovery*, 2008, **7**, 143–155; (*b*) P. Linsel-Nitschke and A. R. Tall, HDL as a target in the treatment of atherosclerotic cardiovascular disease, *Nat. Rev. Drug Discovery*, 2005, **4**, 193–205.

2 M. Wang and M. R. Briggs, HDL: the metabolism, function, and therapeutic importance, *Chem. Rev.*, 2004, **104**, 119–137.

3 (*a*) W. S. Davidson and T. B. Thompson, The structure of apolipoprotein A-I in high density lipoproteins, *J. Biol. Chem.*, 2007, **282**, 22249–22253; (*b*) M. J. Thomas, S. Bhat and M. G. Sorci-Thomas, Three-dimensional models of HDL ApoA-I: implications for its assembly and function, *J. Lipid Res.*, 2008, **49**, 1875–1883; (*c*) P. Sevugan Chetty, L. Mayne, Z. Y. Kan, S. Lund-Katz, S. W. Englander and M. C. Phillips, Apolipoprotein A-I helical structure and stability in discoidal high-density lipoprotein (HDL) particles by hydrogen exchange and mass spectrometry, *Proc. Natl. Acad. Sci. U. S. A.*, 2012, **109**, 11687–11692; (*d*) M. C. Phillips, New insights into the determination of HDL structure by apolipoproteins, *J. Lipid Res.*, 2013, **54**, 2034–2048.

4 (*a*) M. Balestrieri, L. Cigliano, M. L. Simone, B. Dale and P. Abrescia, Haptoglobin inhibits lecithin–cholesterol acyltransferase in human ovarian follicular fluid, *Mol. Reprod. Dev.*, 2001, **59**, 186–191; (*b*) M. S. Spagnuolo, L. Cigliano, L. D. D'Andrea, C. Pedone and P. Abrescia, Assignment of the binding site for haptoglobin on apolipoprotein A-I, *J. Biol. Chem.*, 2005, **280**, 1193–1198.

5 M. G. Sorci-Thomas, L. Curtiss, J. S. Parks, M. J. Thomas, M. W. Kearns and M. Landrum, The hydrophobic face orientation of apolipoprotein A-I amphipathic helix domain 143–164 regulates lecithin–cholesterol acyltransferase activation, *J. Biol. Chem.*, 1998, **273**, 11776–11782.

6 L. Cigliano, C. R. Pugliese, M. S. Spagnuolo, R. Palumbo and P. Abrescia, Haptoglobin binds the antiatherogenic protein apolipoprotein E – impairment of apolipoprotein E stimulation of both lecithin–cholesterol acyltransferase activity and cholesterol uptake by hepatocytes, *FEBS J.*, 2009, **276**, 6158–6171.

7 M. Bucci, L. Cigliano, V. Vellecco, L. D. D'Andrea, B. Ziaco, A. Rossi, L. Sautebin, A. Carlucci, P. Abrescia, C. Pedone, A. Ianaro and G. Cirino, Apolipoprotein A-I (ApoA-I) mimetic peptide P2a by restoring cholesterol esterification unmasks ApoA-I anti-inflammatory endogenous activity in vivo, *J. Pharmacol. Exp. Ther.*, 2012, **340**, 716–722.

8 I. L. Karle and P. Balaram, Structural characteristics of alpha-helical peptide molecules containing Aib residues, *Biochemistry*, 1990, **29**, 6747–6756.

9 D. Bashtovyy, M. K. Jones, G. M. Anantharamaiah and J. P. Segrest, Sequence conservation of apolipoprotein A-I affords novel insights into HDL structure-function, *J. Lipid Res.*, 2011, **52**, 435–450.

10 R. Kaul and P. Balaram, Stereochemical control of peptide folding, *Bioorg. Med. Chem.*, 1999, **7**, 105–117.

11 (*a*) J. D. Tyndall, T. Nall and D. P. Fairlie, Proteases universally recognize beta strands in their active sites, *Chem. Rev.*, 2005, **105**, 973–999; (*b*) C. Toniolo, F. Formaggio, M. Crisma, G. M. Bonora, S. Pegoraro, S. Polinelli, W. H. J. Boesten, H. E. Schoemaker, Q. B. Broxterman and J. Kamphuis, Synthesis, characterization and solution conformational analysis of Cα-methyl, Cα-benzylglycine[(αMe)Phe] model peptides, *Pept. Res.*, 1991, **5**, 56–61.

12 N. J. Greenfield, Using circular dichroism spectra to estimate protein secondary structure, *Nat. Protoc.*, 2007, **1**, 2876–2890.

13 K. Wuthrich, Protein structure determination in solution by nuclear magnetic resonance spectroscopy, *Science*, 1989, **243**, 45–50.

14 D. S. Wishart, B. D. Sykes and F. M. Richards, Relationship between nuclear magnetic resonance chemical shift and protein secondary structure, *J. Mol. Biol.*, 1991, **222**, 311–333.

15 T. Herrmann, P. Guntert and K. Wuthrich, Protein NMR structure determination with automated NOE assignment using the new software CANDID and the torsion angle dynamics algorithm DYANA, *J. Mol. Biol.*, 2002, **319**, 209–227.

16 (*a*) M. Mayer and B. Meyer, Group epitope mapping by saturation transfer difference NMR to identify the segments of a ligand, which is in direct contact with a protein receptor, *J. Am. Chem. Soc.*, 2001, **123**, 6108–6117; (*b*) B. Meyer and T. Peters, NMR spectroscopy techniques for screening and identifying ligand binding to protein receptors, *Angew. Chem., Int. Ed.*, 2003, **42**, 864–890.

17 G. M. Clore and A. M. Gronenborn, Theory of the time dependent transferred nuclear Overhauser effect: application to the structural analysis of ligand–protein complexes in solution, *J. Magn. Reson.*, 1983, **53**, 423–442.

18 A. Kumar, G. Wagner, R. R. Ernst and K. Wutrich, Buildup rates of the nuclear Overhauser effect measured by two-dimensional proton magnetic resonance spectroscopy: implications for the studies of protein conformation, *J. Am. Chem. Soc.*, 1981, **103**, 3654–3658.

19 M. R. Langlois and J. R. Delanghe, Biological and clinical significance of haptoglobin polymorphism in humans, *Clin. Chem.*, 1996, **42**, 1589–1600.

20 N. J. Anthis and G. M. Clore, Sequence-specific determination of protein and peptide concentrations by absorbance at 205 nm, *Protein Sci.*, 2013, **22**, 851–858.

21 T. D. Goddard and D. G. Kneller, *SPARKY 3*, University of California, San Francisco.

22 J. E. Masse and R. Keller, AutoLink: Automated sequential resonance assignment of biopolymers from NMR data by relative-hypothesis-prioritization-based simulated logic, *J. Magn. Reson.*, 2005, **174**, 133–151.

23 R. Koradi, M. Billeter and K. Wuthrich, MOLMOL: a program for the display and analysis of macromolecular structures, *J. Mol. Graphics*, 1996, **14**, 29–32.

24 N. Guex and M. C. Peitsch, SWISS-MODEL and the Swiss-PdbViewer: an environment for comparative protein modeling, *Electrophoresis*, 1997, **18**, 2714–2723.

25 W. R. P. Scott, P. H. Huenenberger, I. G. Tironi, A. E. Mark, S. R. Billeter, J. Fennen, A. E. Torda, T. Huber, P. Krueger and W. F. van Gunsteren, The GROMOS biomolecular simulation program package, *J. Phys. Chem. A*, 1999, **103**, 3596–3607.

26 M. M. Bradford, A rapid and sensitive method for the quantitation of microgram quantities of protein utilizing the principle of protein-dye binding, *Anal. Biochem.*, 1976, **72**, 248–254.

27 L. Cigliano, M. S. Spagnuolo and P. Abrescia, Quantitative variations of the isoforms in haptoglobin 1-2 and 2-2 individual phenotypes, *Arch. Biochem. Biophys.*, 2003, **416**, 227–237.

28 L. Cigliano, L. D. D'Andrea, B. Maresca, M. Serino, A. Carlucci, A. Salvatore, M. S. Spagnuolo, G. Scigliuolo, C. Pedone and P. Abrescia, Relevance of the amino acid conversions L144R (Zaragoza) and L159P (Zavalla) in the apolipoprotein A-I binding site for haptoglobin, *Biol. Chem.*, 2008, **389**, 1421–1426.

29 A. Porta, E. Cassano, M. Balestrieri, M. Bianco, R. Picone, C. De Stefano and P. Abrescia, Haptoglobin transport into human ovarian follicles and its binding to apolipoprotein A-1, *Zygote*, 1999, **7**, 67–77.

30 C. H. Chen and J. J. Albers, Characterization of proteoliposomes containing apoprotein A-I: a new substrate for the measurement of lecithin–cholesterol acyltransferase activity, *J. Lipid Res.*, 1982, **23**, 680–691.